

VEGETATION INDICES, ABOVE GROUND BIOMASS ESTIMATES AND THE RED EDGE FROM MERIS

Frek VAN DER MEER^{1,2}, Wim BAKKER³, Klaas SCHOLTE⁴, Andrew SKIDMORE⁵, Steven DE JONG⁶, Jan CLEVERS⁷, Gerrit EPEMA⁸

¹ITC, Geology Division, Enschede, the Netherlands, vdmeer@itc.nl

²Delft University of Technology, Faculty of Civil Engineering and Geosciences, Delft, The Netherlands, f.d.vandermeer@citg.tudelft.nl

³ITC, Remote Sensing & GIS laboratory, Enschede, the Netherlands, bakker@itc.nl

⁴Joint Research Center, Space Application Institute, Ispra, Italy, klaas.scholte@jrc.it

⁵ITC, Agriculture, Conservation and Ecology division, Enschede, the Netherlands, skidmore@itc.nl

⁶University of Utrecht, Department of Physical Geography, Utrecht, the Netherlands, s.dejong@geog.uu.nl

⁷Wageningen University and Research Centre, Centre for Geoinformation, Wageningen, The Netherlands, Jan.Clevers@staff.girs.wau.nl

⁸Wageningen University and Research Centre, Centre for Geoinformation, Wageningen, The Netherlands, gerrit.epema@staff.girs.wau.nl

Working Group VII/7

KEY WORDS: Vegetation indices, biomass estimates, red edge, MERIS

ABSTRACT

Within the framework of ESA's Earth Observation Program, the Medium Resolution Imaging Spectrometer (MERIS) is developed as one of the payload components of the ENVISAT-1. MERIS is a fully programmable imaging spectrometer, however a standard 15 channel band set will be transmitted for each 300 m. pixel (over land) covering the visible and near-infrared wavelength range. Since MERIS is a multidisciplinary sensor providing data that can be input into ecosystem models at various scales, we studied MERIS' performance relative to the scale of observation using simulated data sets degraded to various resolutions in the range of 6m. up to 300m. Algorithms to simulate MERIS data using airborne imaging spectrometer data sets are presented, including a case study from DAIS 79-channel imaging spectrometer data acquired on 8 July 1997 over the Le Peyne test site in southern France. For selected target endmembers garrigue, maquis, mixed oak forest, pine forest and bare agricultural field, regions of interest are defined in the DAIS scene. For each of the endmembers, the vegetation index values in the corresponding ROI is calculated for the MERIS data at the spatial resolutions ranging from 6 up to 300m. We applied the NDVI, PVI, WdVI, SAVI, MSAVI, MSAVI2 and GEMI vegetation indices. Above ground biomass was estimated in the field and derived from the DAIS image and the MERIS data sets (6-300m. resolution). The vegetation indices show to be constant with the spatial scale of observation. The best relation between the MERIS' and DAIS' NDVI is obtained when using a linear model with an offset of 0.15 ($r=0.31$). A Pearson correlation matrix between above ground biomass measured in the field and each spectral band reveals a modest but significant ($p<0.05$) correlation for most spectral bands. When mathematical functions are fitted through the NDVI and biomass data, an exponential fit shows the extinction and saturation at larger vegetation biomass values. As the correlation between biomass and NDVI for DAIS is modest, for MERIS imagery hardly a correlation is found ($r = 0.2$). This could imply that the MERIS spatial resolution is too coarse relative to the field sampling scale or that accurate above ground biomass estimates from DAIS (and thus MERIS) imagery are impossible to derive. In the last part of the paper, we show that MERIS can produce reliable red edge positioning information.

1 INTRODUCTION

Within the framework of ESA's Earth Observation Programme, the Medium Resolution Imaging Spectrometer (MERIS; Rast *et al.* 1999) is developed as one of the payload components of the ENVISAT-1, proposed for launch in 2000). MERIS is an advanced optical sensor with high spectral and moderate spatial resolution designed to acquire remote sensing data of relevance to environmental management and to the understanding of regional to global scales (Bézy *et al.*, 1996). MERIS' primary mission goal embraces biophysical oceanography (phytoplankton biomass and productivity) and the secondary mission goals of MERIS include atmospheric investigations as well as land surface

processes. The capabilities of MERIS for oceanic studies have been widely investigated here we study the use of MERIS for land applications. Some work on this topic has been conducted. In this paper we present the results of a study of the MERIS vegetation index and biomass estimates at various spatial scales of observation. MERIS data is simulated using airborne imaging spectrometer data from the DAIS 7915 imager.

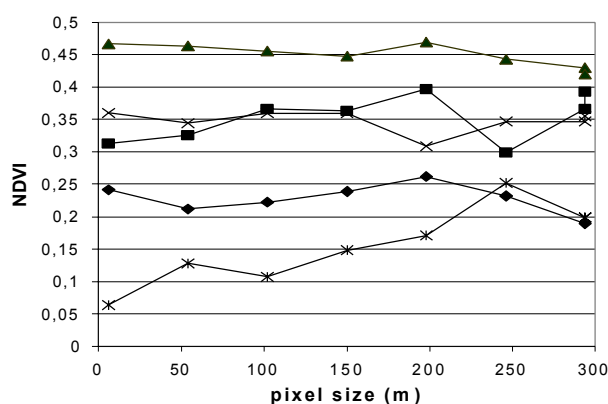


Figure 1. NDVI results emphasizing the spectral domain for garrigue, maquis, mixed oak forest, pine forest and a bare agricultural field (abandoned vine yard, ploughed) at different spatial scales (symbol for the endmembers: garrigue = diamond, maquis = square, mixed oak forest = triangle, pine forest = cross, bare agricultural field = star).

2 MERIS SIMULATION USING DAIS AIRBORNE DATA

Spectral simulation is possible when the source sensor has a spatial and spectral resolution higher and better respectively than the target simulated sensor (Justice *et al.*, 1989). The spectral resampling of existing airborne/spaceborn data sets towards the MERIS spectral properties are not described in detail in the literature. Spatial resampling methods are described by Justice *et al.* (1989). These authors use a spatial filter (gaussian blur filter) and sampling mechanism (Fast Fourier Transforms) to simulate coarse resolution data. We use band matching to simulate MERIS from DAIS. Spatial degradation follows two steps. The first step requires modeling the transfer function between the initial data and the desired data and deriving a spatial filter that allows simulation of the coarse resolution imagery. The second step involves re-sampling to the desired pixel size. As is the case in spectral re-sampling with the

spectral response function, the sensor's Point Spread Function (PSF) gives the spatial response of the sensor. We used as input to the simulation, airborne data from the DAIS 7915 acquired by DLR under the EU TMR-LSF program over the Le Peyne test site (Southern France). The Peyne river is a tributary of the Hérault river and is located in central southern France, roughly between Montpellier and Béziers. The catchment is located at the edge of the Massif Central, the 'Montagne Noir' and the coastal plain of the Mediterranean sea. As a result of this, the Le Peyne catchment displays a large variety of soil and rock types from north to south. The flight lines of DAIS were chosen in such a way that they cover as much as possible variation in geology, soils and vegetation. The physiographic sections that can be distinguished from south-east to north-west are as follows. The southern part consists of Tertiary marl and limestones. The rivers Peyne and Hérault have locally deposited recent fluvial material on top of these formations. Moving north-west Triassic marls and sandy dolomites are surfacing. Next, a complex area of Paleozoic flysch and conglomerates is situated around the artificial lake of Vailhan. The northern part of the DAIS flight strips are covered by Permian reddish clayey marls. At various locations in the study area, basalt and tuff formations are found documenting volcanic activities dated Pliocene. The land use in the southern flat part of the Le Peyne catchment is predominantly vineyards. The northern part is characterized by a hilly terrain covered by a mixed oak forest of Mediterranean sclerophyllous species.

The 79-channel Digital Airborne Imaging Spectrometer (DAIS 7915) built by the Geophysical Environmental Research corp. (GER) is the successor of the 63-channel imaging spectrometer GERIS. The instrument covers the spectral range from the visible to the thermal infrared wavelengths at variable spatial resolution from 3 to 20 m. depending on the carrier aircraft flight altitude. Six spectral channels in the 8 - 12 μm . The DAIS images were calibrated by DLR and delivered within units of radiance. The radiometric correction was done using the empirical line method with dolomite, water, bauxite and a bare agricultural field spectrum as targets. Geometric correction was conducted using a new geostatistical approach that employs a moving neighbourhood kriging. Kriging is applied to predict ground control

points from a set of measured differential GPS samples in the field. Usually airborne datasets are not oriented towards the north because of disk space requirements, but rather stored in a file in the flight direction of the aircraft.

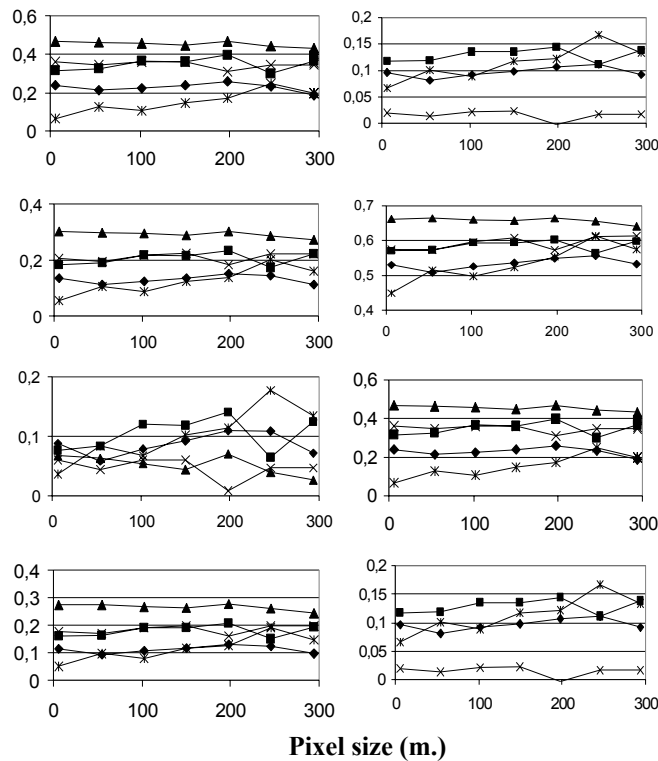


Figure 2. Vegetation indices for different target types at different spatial resolutions ranging from 6m. up to 294 m. (from top left to bottom right: NDVI, WdVI, SAVI, GEMI, TSAVI, PVI, MSAVI2, MSAVI, symbol for the endmembers: garrigue = diamond, maquis = square, mixed oak forest = triangle, pine forest = cross, bare agricultural field = star).

3 MERIS VEGETATION INDICES

Five regions of interest (ROI) were defined in the DAIS scene for selected target endmembers: garrigue, maquis, mixed oak forest, pine forest and bare agricultural field. For each of these endmembers the vegetation index values were calculated using the following equations, respectively:

$$NDVI = \frac{NIR - red}{NIR + red} \quad [1]$$

$$PVI = \frac{1}{\sqrt{a^2 + 1}} * (NIR - a * r - b) \quad [2]$$

$$WdVI = NIR - a * red \quad [3]$$

$$SAVI = \frac{NIR - red}{NIR + red + L} * (1 + L) \quad [4]$$

$$TSAVI = \frac{a * (NIR - a * red - b)}{(b * NIR + red - b * a + X * (1 + a * a))} \quad [5]$$

$$MSAVI = \frac{NIR - red}{NIR + red + (1 - 2 * a * NDVI * WdVI)} \quad [6]$$

$$\text{MSAVI2} = \frac{2NIR + 1 - \sqrt{(2NIR + 1)^2 - 8(NIR - red)}}{2} \quad [7]$$

$$\text{GEMI} = \left[\frac{red - 0.125}{1 - red} \right] \cdot \left[\frac{2NIR + 1 - \sqrt{(2NIR + 1)^2 - 8(NIR - red)}}{2} \right] \quad [8]$$

where NIR is the near infrared reflectance (MERIS band 12 at 775nm., DAIS band 17 at 773nm.), red is the red reflectance (MERIS band 7 at 665nm., DAIS band 11 at 671nm.), a is the slope angle between the soil line and the near infrared axis, b is the offset of the soil line, X is the x factor described earlier, L is the L factor described earlier, and eta is defined as

$$eta = \frac{2 * [(NIR)^2 - red]^2 + (1.5 * NIR) + (0.5 * red)}{NIR + red + 0.5} \quad [9]$$

Biomass estimates were derived in the field from 120 transects of 30 meters. For shrubs, the method of Pereira *et al.* (1993) was used which applies the following formula to calculate biomass:

$$shrubs = 0.642 * (h_s)^{0.075} * (d_s)^{2.4901} * 166.67 * N_s \quad [10]$$

For trees we used the method of Floret *et al.* (1989) which applies the following equation:

$$trees = \frac{(-16.6845 + (0.65729(d_t)^2 * h_t)) * N_t}{6} \quad [11]$$

where h is height in cm., d is diameter in cm. and N is the counts. To assess above ground biomass (AGB) from spectral information a spreadsheet database was created with geographic co-ordinates, cover types and AGB for trees, shrubs and their totals. All sample points were located in the DAIS and MERIS imagery and were added to the database. The database allowed statistical analysis of the spectral and biomass information, which enabled to create transfer models to assess AGB from spectral information.

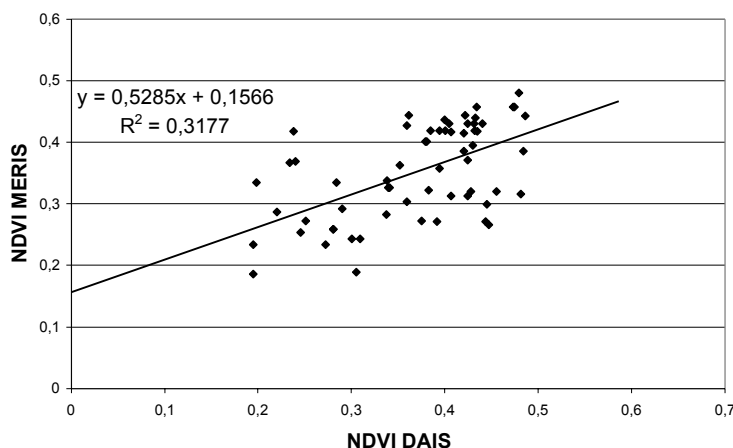


Figure 3. Relation between DAIS NDVI and MERIS NDVI with $y=x$ plot line offset by 0.15 yielding the best possible (but statistically insignificant) fit.

4 RESULTS OF VEGETATION INDEX AND BIOMASS ESTIMATES

Comparing the different vegetation index values from the different ROIs at the different spatial scales (Figure 1 and 2) the following can be seen: the vegetation indices remain constant at all scales. As mixed oak forest is thought to cover the surface close to 100%, this ROI should give the highest vegetation index values. The garrigue endmember is thought to have the lowest value. Vegetation index values derived from the NDVI, SAVI, MSAVI, MSAVI2 and GEMI confirm this. The GEMI, however, has much higher values than the other indices. This maybe the result from the objective of the GEMI: to correct for atmospheric interactions. Alternatively, the radiometric calibration of the DAIS7915 image using the empirical line method is not sufficient. Figure 2 shows that the PVI, WdVI and TSAVI show a pattern contrary to that of the other vegetation indices. For these indices, mixed oak forest has the lowest vegetation index values and garrigue the highest. The PVI is an atmospheric sensitive index, and described above, a detailed look should be given to the accuracy of the performed radiometric calibration. The WdVI is calculated using a

soil line which might have been wrongly defined. The TSAVI is calculated using a soil adjustment factor X . This X -factor used (0.08) and may not be appropriate in our specific case. The curves show some irregularities, in some cases vegetation index values increase with increasing pixel size, sometimes vegetation index values decrease. Especially around the 250 m. pixel size, the maquis and the agricultural field values become very erratic. Pine vegetation index values show a decrease at 200 m. pixel size, while the other types still have increasing values.

Figure 1 illustrates the relation between NDVI and pixel size for the five different target types garrigue, maquis, mixed oak forest, pine forest and a bare agricultural field (i.e., an abandoned and ploughed vine yard). For four defined targets varying spatial resolution from 6 up to 300 m. has no effect on the NDVI and the curves are almost superimposed and distinct NDVI amplitudes can be seen. Mixed oak forest has the highest NDVI level (approximately 0.45), maquis and pine forest balance around 0.35, garrigue has values between 0.2-0.25 and the bare soil varies between 0.05 and 0.2. The NDVI for the end member bare agricultural field tends to converge towards garrigue at larger spatial resolution due to the problem of not "seeing" a single agricultural field (spatial size: 120x180 m) at the MERIS spatial resolution of 300 m. The relation between the MERIS' and DAIS' NDVI is important because it relates to the spatial correlation between them. In theory one expects to fit a $y=x$ linear through the data (Figure 3), however the best fit ($r=0.31$) is obtained adding an offset of 0.15. A Pearson correlation between biomass and each spectral band reveals a modest but significant ($p<0.05$) correlation for most spectral bands from 0.32-0.44 (DeJong *et al.*, 1998). When mathematical functions are fitted through these data of NDVI and biomass, an exponential fit provides the best result. As expected each fit has the shape of an extinction function and becomes saturated at larger vegetation biomass values (Figure 4). As the correlation between biomass and NDVI for DAIS is modest, for MERIS imagery hardly a correlation exists ($r = 0.2$). There are two possible causes for this (assuming the field measurements to be correct): 1) the MERIS spatial resolution is too coarse according to the field sampling scale or, 2) accurate AGB assessment is difficult (impossible) using DAIS (and thus MERIS) imagery.

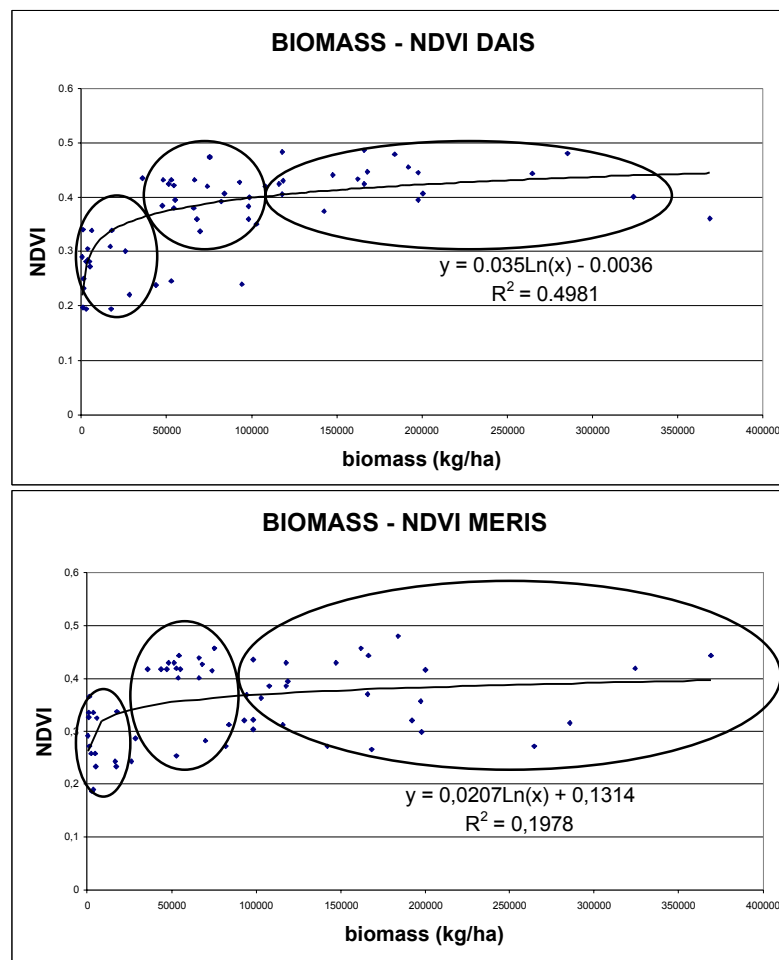


Figure 4. Biomass assessment (AGB) using the original DAIS data (top graph) and the MERIS data (bottom graph). Ellipses (from left to right) identify pixels belonging to the targets.

5 RED EDGE POSITIONING ALGORITHMS FOR MERIS

Two methods for estimating the red edge position of the vegetation spectrum, indicative for plant vitality, are in use: the method of Guyot & Baret (1988) and the method of Dawson & Curran (1998). The linear method is used here (Guyot & Baret 1988) assumes a straight slope of the reflectance spectrum around the midpoint between the reflectance at the NIR plateau and the reflectance minimum at the chlorophyll absorption feature in the red. This midpoint is then defined as the red edge index. This point may not coincide with the maximum of the first derivative, but it appears to be a very robust definition and it needs only a very limited number of spectral bands. Thus, this method is very useful for practical applications. Although the spectral bands of the MERIS standard band setting at the red edge slope are not optimally located, they can be used for applying the linear method for red edge index estimation. The bands to be used are located at 705 and 753.75 nm. However, since the latter band is located very close to the oxygen absorption feature of the atmosphere, an atmospheric correction must be applied previous to calculating the position of the red edge using the MERIS bands. Previous studies have shown that for bands located at about 700 and 740 nm, an atmospheric correction is not necessary since the red edge calculated in terms of reflectances equals the one calculated in terms of radiances. In Figure 5 a comparison of the red edge position calculated using the linear method interpolating between 700 and 740 nm and the linear method using the MERIS spectral bands is shown, thus interpolating between 705 and 754 nm, PROSPECT-SAIL simulation for a canopy with varying leaf chlorophyll content and various LAI values. The regression line $re_{MERIS} = -409.0 + 1.574 * re_{700-740}$ is also plotted providing insight into the statistical viability of the data.

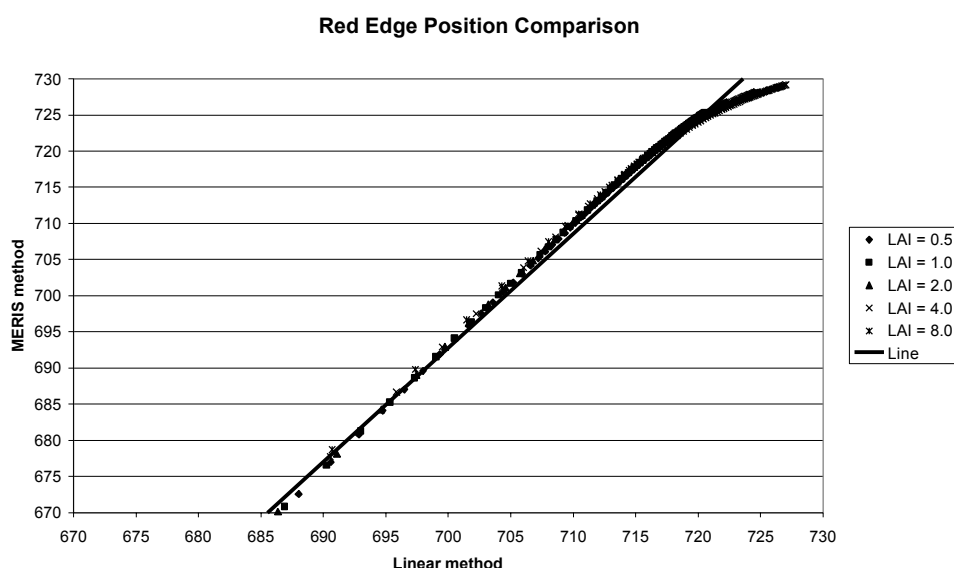


Figure 5. Comparison of the red edge position calculated using the linear method interpolating between 700 and 740 nm and the linear method using the MERIS spectral bands, thus interpolating between 705 and 754 nm, PROSPECT-SAIL simulation for a canopy with varying leaf chlorophyll content and various LAI values. The regression line $re_{MERIS} = -409.0 + 1.574 * re_{700-740}$ is also plotted.

Results in this study show that there exists a nearly linear relationship for the linear method using either bands at about 700 and 740 nm or the MERIS bands, albeit that it not coincides with the 1:1 line. This means that we have to work with instrument-specific red edge indices. For MERIS, the above-mentioned linear relationship may be used for translating red edge index values obtained with one method (using the MERIS bands) into values obtained with the other method (based on bands at 700 and 740 nm). Deviations occur mainly at high red edge index values matching vegetation with a high chlorophyll content and with very high LAI values. To cope with this a non-linear function might be fitted. Another possibility is to fit a second linear relationship for the upper part of the curve. The breakpoint then seems to lie at about 720 nm for the standard linear method (coinciding with about 725 nm for the MERIS method). When fitting a linear function for this upper part of the curve (for the simulated data), the regression line yields $re_{MERIS} = -243.7 + 0.668 * re_{700-740}$ $r = 0.980$. For the remaining part of the curve still the relationship given in the previous section will be used. The two regression lines are illustrated in figure 6. It appears, moreover, that the determination of the red edge index using the MERIS band setting becomes less sensitive to variations in chlorophyll content and LAI than the standard linear method using interpolation between 700 and 740 nm.

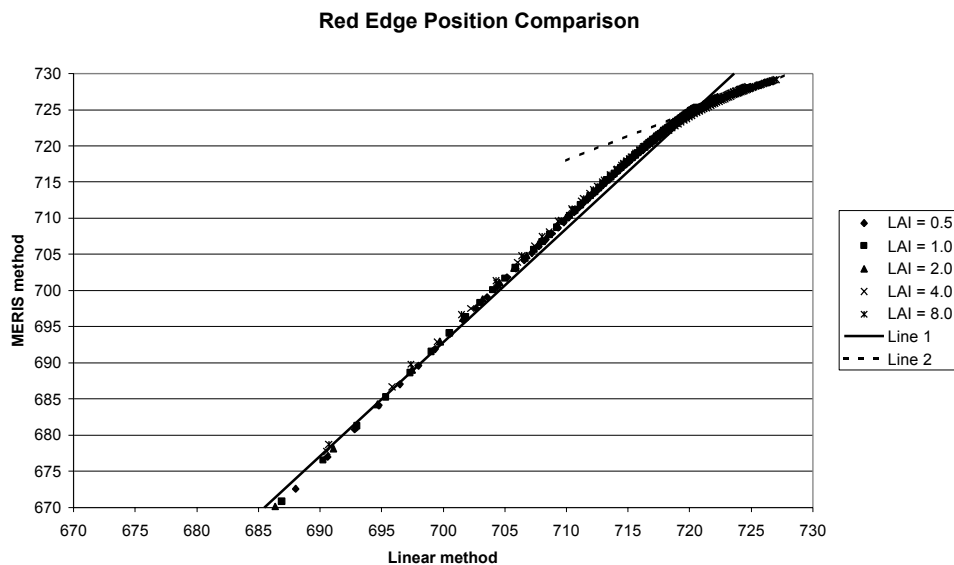


Figure 6. Comparison of the red edge position calculated using the linear method interpolating between 700 and 740m and the linear method using the MERIS spectral bands, thus interpolating between 705 and 754m, PROSPECT-SAIL simulation for a canopy with varying leaf chlorophyll content and various LAI values. The two regression are also plotted: Line 1: $re_{MERIS} = -409.0 + 1.574 * re_{700-740}$ Line 2: $re_{MERIS} = -243.7 + 0.668 * re_{700-740}$

6 CONCLUSIONS

Simulated MERIS data from airborne DAIS data have been presented as well as an approach for the convolution necessary to obtain the data sets. We have gathered biomass data in the field partly from spectral measurements and have derived standard vegetation products from the image data at variable spatial resolutions. Five regions of interest were defined for the selected target endmember: garrigue, maquis, mixed oak forest, pine forest and bare agricultural field. The vegetation indices, although they differ amongst themselves, show to be remarkable constant with the spatial scale of observation. The NDVI for the endmember bare agricultural field tends to converge towards garrigue at larger spatial resolution due to the problem of “seeing” a single agricultural field (spatial size: 120x180 m) at the MERIS spatial resolution of 300 m. A Pearson correlation matrix between above ground biomass measured in the field and each spectral band reveals a modest but significant ($p < 0.05$) correlation for most spectral bands (DeJong *et al.*, 1998). When mathematical functions are fitted through the NDVI and biomass data, an exponential fit gives the best fit showing the extinction and saturation at larger vegetation biomass values. As the correlation between biomass and NDVI for DAIS is modest, for MERIS imagery hardly a correlation is found ($r = 0.2$). There are two possible causes for these results assuming the field measurements are correct and accurate: (1) the MERIS spatial resolution is too coarse relative to the field sampling scale or, (2) accurate above ground biomass estimates from DAIS (and thus MERIS) imagery are impossible to derive. This study has also shown that the MERIS standard band setting can be used for deriving red edge index values. It has paid no attention to the physical interpretation of red edge index values at the scale level of MERIS. The spatial resolution of MERIS is 300 m, so one hardly will observe single fields or objects of just one vegetation type. MERIS application concerns more the application at, for instance, the ecosystem level. Highest sensitivity to variations in vegetation variables, like chlorophyll content and LAI, occurs at the lower values of these variables. One may expect these ranges in variables more at the ecosystem level, particularly when looking at natural ecosystems.

ACKNOWLEDGEMENTS

This research is conducted as part of the MERILand project funded by the Netherlands Remote Sensing Board (BCRS) under contract 3.1/AP-06. Advice by Mike Rast and Steve Delwart (ESA-ESTEC) and Ingrid Janssen (BCRS) was highly appreciated. DAIS data over the Le Payne test site were kindly provided under the DEMON project. We thank Stefan Sommer and Joachim Hill for their assistance. Andreas Mueller, Peter Strobl, Andrea Haushold, Rolf Richter, Franz Lanzl and many others from DLR are thanked for their excellent work during the 1996-1998 DAIS LSF campaigns. Peter Strobl is thanked for his advice on the data calibration. Spectra and biomass data were collected

within the framework of the MERILand field campaign in 1998. Spectra are partly derived from the MERISPECdata base. We thank Stefan Sommer, Helen Preissler, Herve Bohbot of JRC for excellent collaboration on the MERISPEC spectral database.

REFERENCES

- Bézy, J.L., Rast, M., Delwart, S., Merheim-Kealy P. & Bruzzi, S. 1996. The ESA Medium Resolution Imaging Spectrometer (MERIS). *Backscatter* 7(3), pp. 14-19.
- Dawson, T.P., and Curran, P.J., 1998, A new technique for interpolating the reflectance red edge position. *International Journal of Remote Sensing*, 19, pp. 2133-2139.
- De Jong, S.M., Scholte, K., van der Meer, F., Sommer, S. & Lacaze, B. 1998. The DAIS7915 La Peyne experiment: using airborne imaging spectrometry for land degradation survey and modeling. In: *Operational remote sensing for Sustainable Development*. G.J.A. Nieuwenhuis, R.A. Vaughan and M. Molenaar (eds.), A.A. Balkema, Rotterdam: pp. 247-253.
- Guyot, G., and Baret, F., 1988, Utilisation de la haute resolution spectrale pour suivre l'etat des couverts vegetaux. *Proceedings 4th Int. Coll. "Spectral Signatures of Objects in Remote Sensing"*, Aussois, France, ESA SP-287, pp. 279-286.
- Floret C., Galan, M.J., Le Floch, E., Rapp, M. & Romane, F. 1989. Organisation de la Structure, de la Biomasse et de la Minéralomasse d'un Taillis Overt de Chêne Vert (*Quercus ilex* L.) *Acta Oecologica*, 10, pp. 245-262.
- Justice, C.O., Markham, B.L., Townshend, J.R.G. & Kennard, R.L. 1989. Spatial degradation of satellite data. *International Journal of Remote Sensing*, 10(9), pp. 1539-1561.
- Pereira J.M.C., Oliviera, T.M. & Paúl, C.P. 1993. Fuel Mapping in a Mediterranean Shrubland Using Landsat TM imagery. In: *Satellite Technology and GIS for Mediterranean Forest Mapping and Fire Management*, P.J. Kennedy and M. Karteris (eds.), Technical JRC Report EUR15861 EN: pp. 97-106.
- Rast, M., Bézy, J.L. & Bruzzi, S. 1999. The ESA Medium Resolution Imaging Spectrometer MERIS – a review of the instrument and its mission. *International Journal of Remote Sensing*, 20, pp. 1681-1702.